Elevated temperature creep deformation of a single crystal superalloy through the small punch creep method

S. P. Jeffs [a,*], R. J. Lancaster [a]

[a] *Institute of Structural Materials, College of Engineering, Swansea University, Singleton Park, Swansea, SA2 8PP*
[*] *Corresponding author: Dr S.P. Jeffs; Tel: +441792602061; Fax: +441792295693; Email address: s.p.jeffs@swansea.ac.uk*

Abstract
Small punch testing is now a widely recognised approach for obtaining useful mechanical property information of critical structural components, particularly in the nuclear industry. However, to date the utilisation of this method has been limited to isotropic materials such as aluminium alloys and steels. This paper will look to utilise the small punch (SP) test to assess the creep response of <001>-orientated CMSX-4® at temperatures above 950°C. An orthogonal rafting regime of the γ' structure is observed in the post-test microstructure due to the biaxial tension state typically produced in a SP test. Interpretation of the SP results to correlate with uniaxial creep data is carried out by employing the k_{sp} approach in order to provide a platform for future material assessment.

1. Introduction

The Small Punch (SP) test technique was initially developed by the nuclear industry in the 1980s to estimate the residual life of components subjected to hostile in-service environments [1]. Since then, the approach has been adopted by many other industrial sectors due to the numerous benefits that the test can offer. Indeed, many of the advantages of this approach relates to the small volume of test material typically required and the significant cost savings that it can potentially offer, whilst producing important creep and fracture data on the respective material. The techniques have now been further developed across worldwide laboratories to obtain creep rupture and tensile fracture data over a range of material systems including steels, titanium and aluminium alloys [2–6]. The method has also proved useful for determining the mechanical properties of discrete locations within components or parts, such as weldments, heat affected zones (HAZs), coatings and interfaces [7]. Extensive use of the SP technique has led to the publication of a European Code of Practice (CoP) in order to standardise SP testing and its application [4]. In addition, the SP CoP also proposes a SP creep correlation factor, k_{sp}, where the SP load may be correlated to a uniaxial creep stress in order to compare SP and conventional creep data. This approach has been applied across more than one material system [5-6], [8].

Published literature has shown how SP testing can be utilised as an effective tool for ranking creep properties of novel alloy variants in comparison to more traditional uniaxial approaches and also components fabricated through advanced manufacturing processes [9–11]. However, there is limited research currently available that explores the feasibility of SP testing in nickel alloy systems, particularly single crystals, and at extreme temperatures.

Development of experimental single crystal alloys is inherently expensive with an extensive test programme typically required in order to determine the creep properties of the next generation materials. As such the SP creep test provides a cost effective tool for down selection of novel alloy variants. Primarily, the SP creep test has been employed to access the properties of more isotropic materials with little research into anisotropic materials. However, single crystal alloys typically exhibit a strong anisotropic behaviour, whereby the mechanical properties have a high dependency on the orientation, and therefore, the tested orientation of the material. Experimental studies using conventional creep test methods on single crystals have found at intermediate temperatures, in the region of 700°C, [001] orientated crystals typically exhibit the strongest creep resistance, followed by crystals loaded in the [011] orientation and lastly [111], where the effect is most pronounced during the primary creep phase [12–14]. However, at more elevated temperatures, greater than 980°C, which are consistent with in service high pressure turbine conditions of jet engine systems, creep behaviour has been found to be more isotropic than at lower temperatures [12]. For example, at 760°C with an applied stress of 750MPa, the creep rupture life of [001] orientated crystals is 1138 hours, compared to 36 hours in the [111] orientation. On the other hand, at 1050°C and 120MPa, [001] orientated crystals exhibit a creep life between 468-705 hours, [011] orientation a life of 536 hours and [111] orientated crystals a life of 474-682 hours [12].

This research assesses the suitability of the SP creep test method in determining the elevated temperature creep properties of the nickel based single crystal superalloy, CMSX-4, and correlates the results with those produced through more conventional uniaxial approaches. The microstructural evolution throughout the SP test is interpreted, notably the difference in the configuration of rafting, in comparison to the conventional microstructural response derived from uniaxial techniques.

2. Experimental procedure

2.1 Small Punch Creep Test

A series of small punch creep tests were performed on a bespoke high temperature SP creep frame developed at Swansea University, a schematic for which is depicted in Figure 1. In a similar manner to many other established approaches [15], loading was typically applied through the central axis of the rig via an upper load pan arrangement. This load was directly

applied to a miniature disc sample through the use of a 2mm diameter hemispherical ended ceramic punch and the disc is clamped within an upper and lower die to prevent any residual flexing motion. The specimen was located centrally within a furnace, and was encased by a ceramic tube to provide an inert argon atmosphere in order to eliminate any potential oxidation effects. To avoid argon leakage, cooling jackets were fitted at either end with PTFE seals to aid retention of frictional contact between the jacket and the tube, and to ensure a hermetic seal for the argon. Heat was applied using a digitally controlled furnace and was constantly monitored throughout the test by two Type N thermocouples located in a drilled hole in the upper die, close to the surface of the disc.

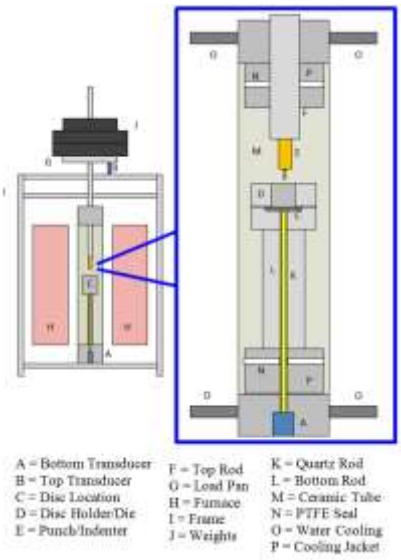

Figure 1 - Bespoke high temperature SP creep rig

Due to the significant creep strength of the tested material, a number of punch designs and materials were trialled for this research. These included tungsten carbide, zirconia and alumina, in the traditional 2mm diameter hemi-spherically ended punch design. The tungsten carbide indenter in this design was initially trialled and was found to flatten and buckle under the high loads and elevated temperatures required for this series of experiments. As such, zirconia and alumina ceramic punches were employed since they possess superior compressive strengths and elevated temperature properties. The results obtained from this arrangement were found to be of a high quality. However, due to the ductility of the tested material, as the central ligament of the specimen elongates under the applied load, the material envelopes around the tip of the punch which then detaches post test. This led to the development and introduction of a two piece punch design, consisting of a concave ended tip and a sacrificial 2mm diameter ball, in order to minimise the cost from test to test. As such, all tests were performed with alumina and zirconia indenters in the 2 piece configuration.

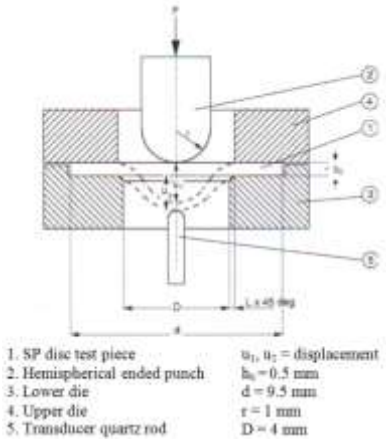

Figure 2 - SP test piece geometry showing the deformation of the SP disc [4]

All SP creep tests were performed in accordance with the European CoP [4], from which a schematic of the typical test dimensions are shown in Figure 2, where a 2mm diameter hemi-spherically tipped indenter, albeit via a 2mm diameter ball, was utilised in conjunction with a 4mm receiving hole. Disc displacement was measured through upper and lower linear variable displacement transducers (LVDT) where the upper LVDT was attached directly beneath the load pan and monitors the depth that the indenter penetrates into the top surface of the disc, whereas the lower transducer measures the deflection

from the underside of the SP specimen via a quartz rod. Data was recorded after regular intervals through a dedicated Dirlik Control logging system.

An important consideration for SP testing at such elevated temperatures are the thermal stresses that may result from the clamped configuration that holds the SP miniature disc specimen in place. As such, miniature discs of CMSX-4 were clamped in the Nimonic 90 die set, and therefore, the difference in magnitude of the thermal expansion coefficients requires consideration. At 1000°C the difference in linear thermal expansion is ~2.73×10^{-6} $°C^{-1}$, so for [001] orientated CMSX-4 possessing a modulus value of approximately 80GPa [16], a tensile stress of 218MPa would typically be produced in all radial directions in which the specimen is clamped. It is suggested that these thermal stresses result in additional creep strain, which would be expected to be consistent from test to test.

2.2 Material

The material under investigation for this research was the second generation nickel based single crystal superalloy, CMSX-4, which is regarded as the material of choice for high pressure turbine blade applications in gas turbine engines. Following casting the alloy was solution treated at 1312°C, gas-fan quenched, primary aged at 1150°C, quenched and finally aged at 870°C. The composition of CMSX-4 is summarised in Table 1 and the corresponding microstructure from Scanning Electron Microscopy (SEM) is displayed in Figure 3. Additional microstructural measurements regarding the typical widths of the γ channels and the γ' precipitates are displayed in Table 2.

Table 1 - Alloy Composition (wt%)

	Co	Cr	Mo	W	Re	Al	Ti	Ta	Hf
CMSX-4	9	6.4	0.6	6.4	3	5.6	1	6.5	0.1

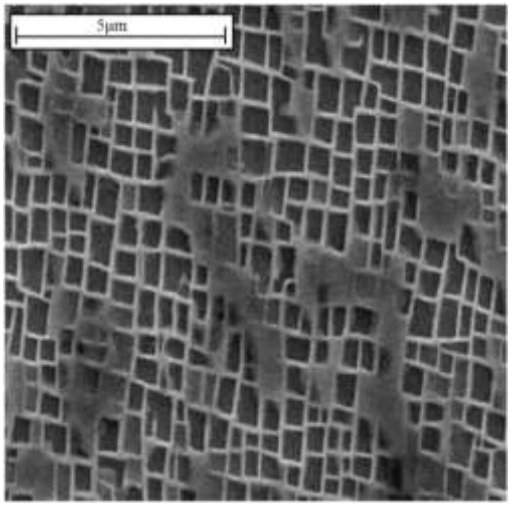

Figure 3 - SEM microstructure of CMSX-4

Table 2 - Microstructural Measurements

	Average width of γ' (μm)	Average width of γ channels (μm)
CMSX-4	0.45	0.15

Cylindrical rods of CMSX-4 were cast within 15° of the [001] orientation. The rods were turned down to 9.5mm diameter and SP specimens were prepared by sectioning slices ~800μm in thickness and ground with progressively finer papers until a 500μm ± 5μm thickness was achieved, in accordance with the SP code of practice [4].

Figure 4 shows the diagrammatic representation of the biaxial tension state during a SP creep test with the FCC unit cell for CMSX-4, showing that stress occurs in two directions on the plane orthogonal to the [001] loading direction, thus encompassing the [100], [010] and [110] orientations.

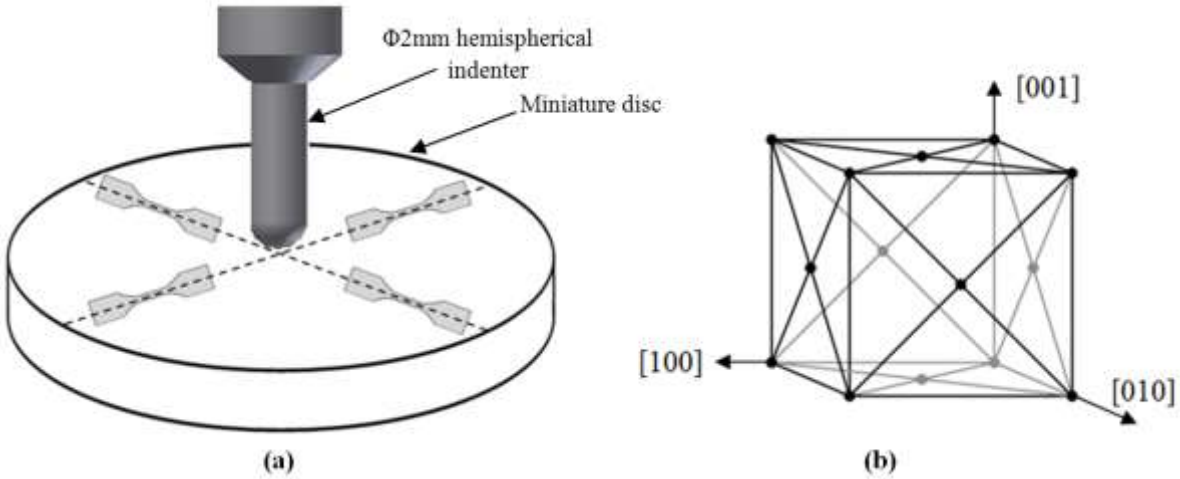

Figure 4 - Representation of (a) the bi-axial tension deformation behaviour on a SP creep specimen and (b) corresponding FCC unit cell of CMSX-4

3. Results and Discussion

Figure 5 illustrates the typical experimental data generated at 950°C under SP conditions. The data shows that the SP test provides an effective method for distinguishing the sensitivity of CMSX-4 to load at high temperature, where the highest induced load yields the shortest time to rupture. This response is also comparable to that seen of traditional uniaxial creep test methods, with an initial decaying displacement rate during primary type deformation, followed by an accelerating tertiary phase during which the creep rate increases. Following the success of the SP method at 950°C, investigation into how the technique distinguishes the sensitivity of temperature was carried out.

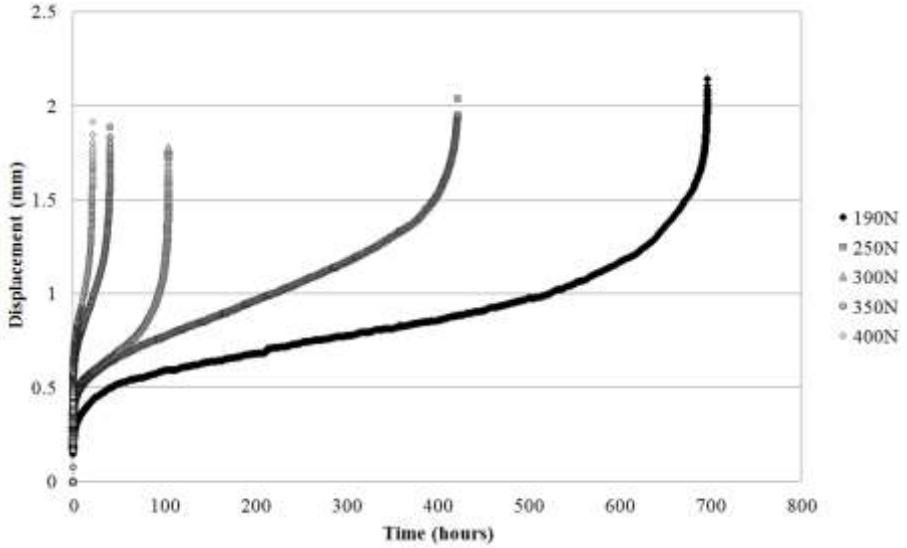

Figure 5 - SP creep curves for CMSX-4 at 950°C at a range of applied loads

Figure 6 shows the rupture life response for SP creep tests of [001] orientated CMSX-4 at the three temperatures; 950°C, 1050°C and 1150°C, with loads varying from 75N to 400N. A strong relationship is clearly identifiable within the results, demonstrating the effectiveness of the SP method in establishing sensitivity to both load and temperature for a single crystal material at these temperatures. This strong correlation for temperature and loading is further demonstrated in Figure 7, which displays the minimum displacement rate behaviour for the same results.

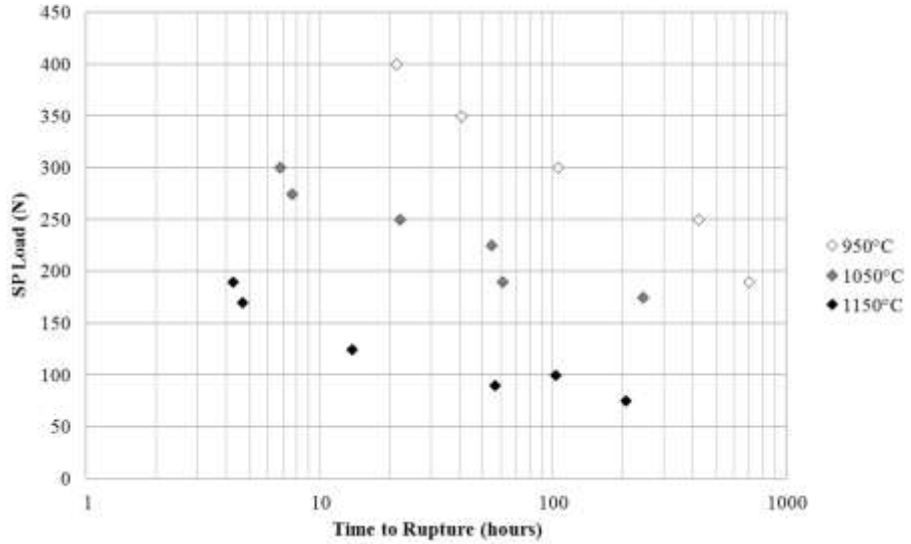

Figure 6 - Load vs. Time to Rupture for SP Creep tests at 950°C, 1050°C and 1150°C

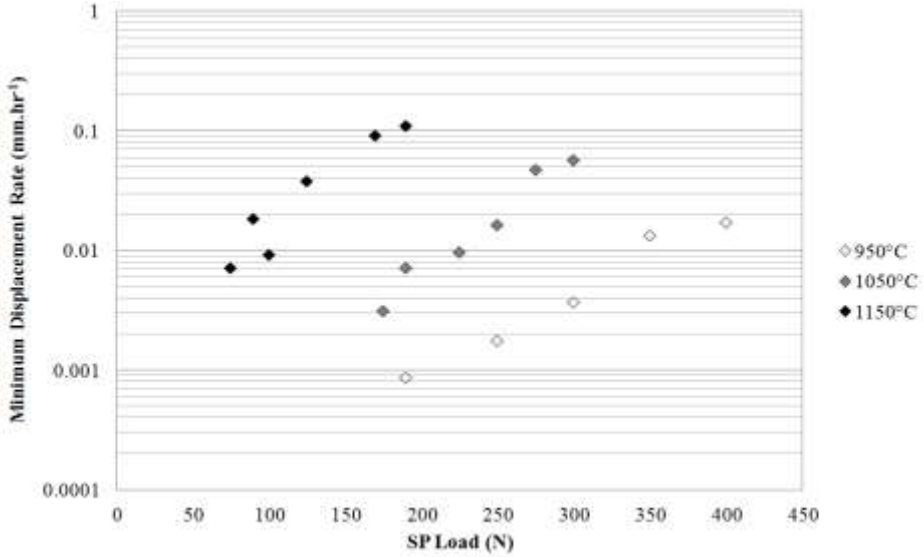

Figure 7 - Minimum Displacement Rate vs. Load behaviour for SP creep of CMSX-4

The ability to correlate SP creep results with conventional uniaxial data is an important factor when considering the benefits of the SP technique, particularly in allowing for cost savings in intensive characterisation programmes of novel materials. The correlation between SP loading in Newtons and uniaxial stress in MPa can be achieved by employing the k_{sp} method, which is detailed within the European Code of Practice [4]. The relationship behaves as follows:

$$\frac{F}{\sigma} = 3.33 k_{sp} R^{-0.2} r^{1.2} h_0$$

Where F is the SP load, σ is the stress applied in a uniaxial creep test, R is the radius of the receiving hole (2mm), r is the radius of the punch indenter (1mm) and h_0 is the test piece thickness (0.5mm).

A key restriction in adopting this approach for single crystal alloys is the inherent anisotropic nature of the material and the variation in creep performance it encourages. However, as previously mentioned, this anisotropic behaviour has been shown to be reduced at elevated temperatures, particularly between [001] and [110] orientations [12]. In a SP creep test, the miniature disc specimen typically deforms via a biaxial tension state, which for this research is recognised as deformation through the [010], [100] and [110] orientations, whereas conventional creep is typically restricted to deformation in a single uniaxial orientation. Therefore, the k_{sp} method can be implemented to correlate the SP creep results against uniaxial data obtained from constant load creep tests on [001] orientated CMSX-4 at such elevated temperatures. Nevertheless, intermediate temperature (600-800°C) would require consideration of the anisotropic nature of the material when comparing the two test types. Figure 8 presents the constant load creep test data for [001] orientated CMSX-4 at 950°C and 1050°C.

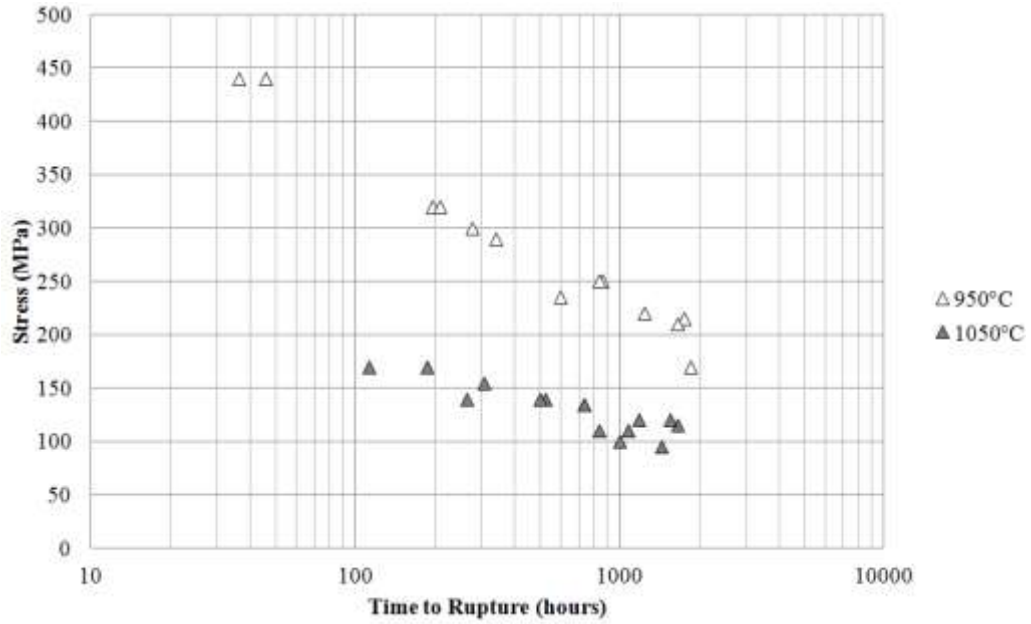

Figure 8 - Uniaxial Creep Data for CMSX-4 at 950°C and 1050°C

Figure 9 plots the stress - time to rupture behaviour for the converted SP tests and the uniaxial constant load creep tests for 950°C and 1050°C. Interestingly the optimal value for the k_{sp} factor is found to be 0.6 for 950°C and 0.8 for 1050°C. The change in k_{sp} at the two temperatures is thought to be due to a microstructural effect which is to be discussed in more detail later. Nevertheless, despite the strong correlation observed between the two different approaches, due to the anisotropic nature of CMSX-4 and the biaxial tension deformation that occurs in a SP creep test, further consideration is necessary in order to confidently determine creep rupture lives of uniaxial CMSX-4 from the SP results.

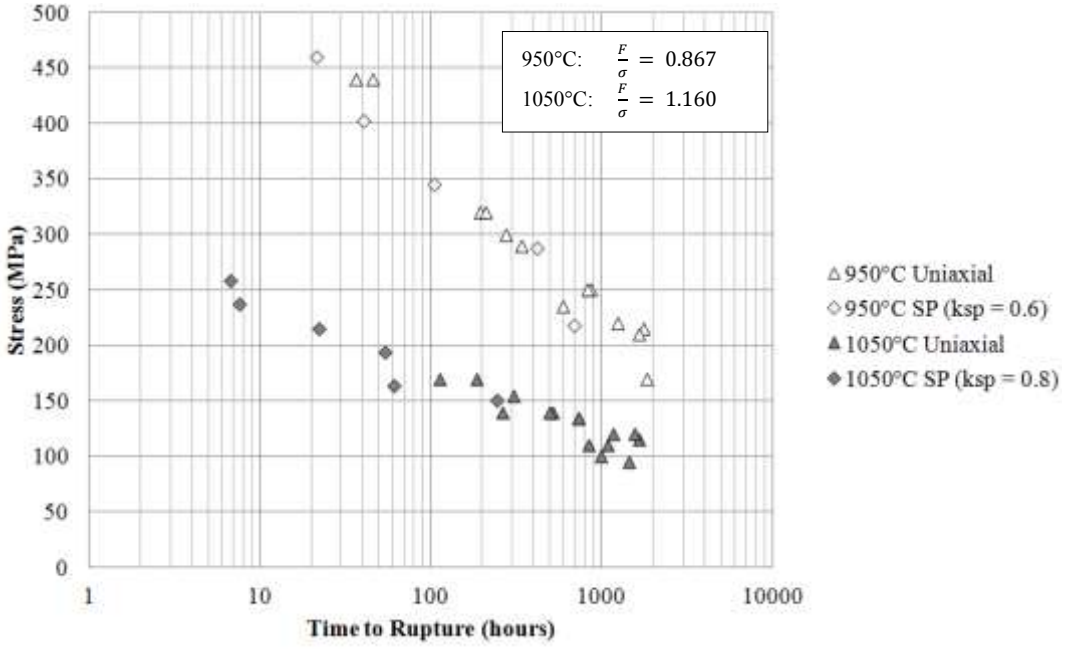

Figure 9 - Stress - Time to Rupture behaviour for uniaxial constant load creep tests and converted SP creep data at 950°C and 1050°C

3.1. Microstructure

At elevated temperatures above 950°C and an applied tensile load, the microstructure of CMSX-4 can evolve from the usual cuboidal γ/γ' configuration to a plate like microstructure [17]. This is directly controlled by two factors that occur in the early stages of creep deformation: (i) equilibrium interfacial dislocation networks forming at the γ/γ' interfaces, and (ii) the γ' particles coalescing by a process of directional coarsening known as the rafting effect [18]. The influence of rafting has previously been reported in uniaxial creep work by Reed *et al* [19]. The rafting effect on creep life however, is not fully

understood since under lower applied stress values, where creep life is typically expected to be long, rafting can actually have a detrimental effect on rupture life. At the same time, rafting is also considered to be partially responsible for the creep-hardening effect which initially occurs and the plateau that transpires thereafter [18].

Figure 10 and 11 illustrate the unique rafting behaviour that occurs in a SP creep disc in comparison to more conventional rafting that is typically observed in a uniaxial creep specimen of CMSX-4. In the uniaxial creep test, the specimen was exposed to a temperature of 1050°C and tested at 140MPa for 300 hours [20]. In this instance, rafting can be seen to occur in a single orientation perpendicular to the applied stress. However, under SP loading rafting develops in two directions perpendicular to one another, as illustrated in Figure 11(b) and (c). These orientations are typically configured in an orthogonal arrangement around the [001] orientation of growth, through which the SP load is exerted. EBSD analysis confirmed that the orientations were [010] & [100], which compliments previous research of [011] orientated uniaxial creep specimens, where the resulting γ' rafts were inclined at 45° thus indicating that growth is promoted along the cube axis [21]. Interestingly, there is an intermediate area of orthogonal orientation of rafted structure at the 'corner' of the [010] and [100] orientations, as illustrated in Figure 11(d). This phenomenon is thought to occur due to the biaxial tensile state that occurs in SP creep testing, as shown originally in Figure 4.

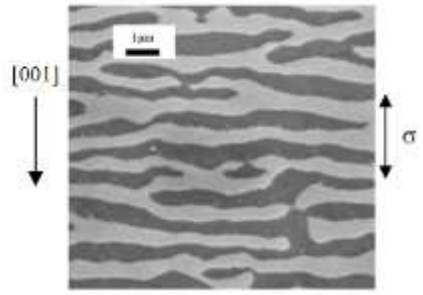

Figure 10 - Rafted microstructure of CMSX-4 from a uniaxial creep specimen [20]

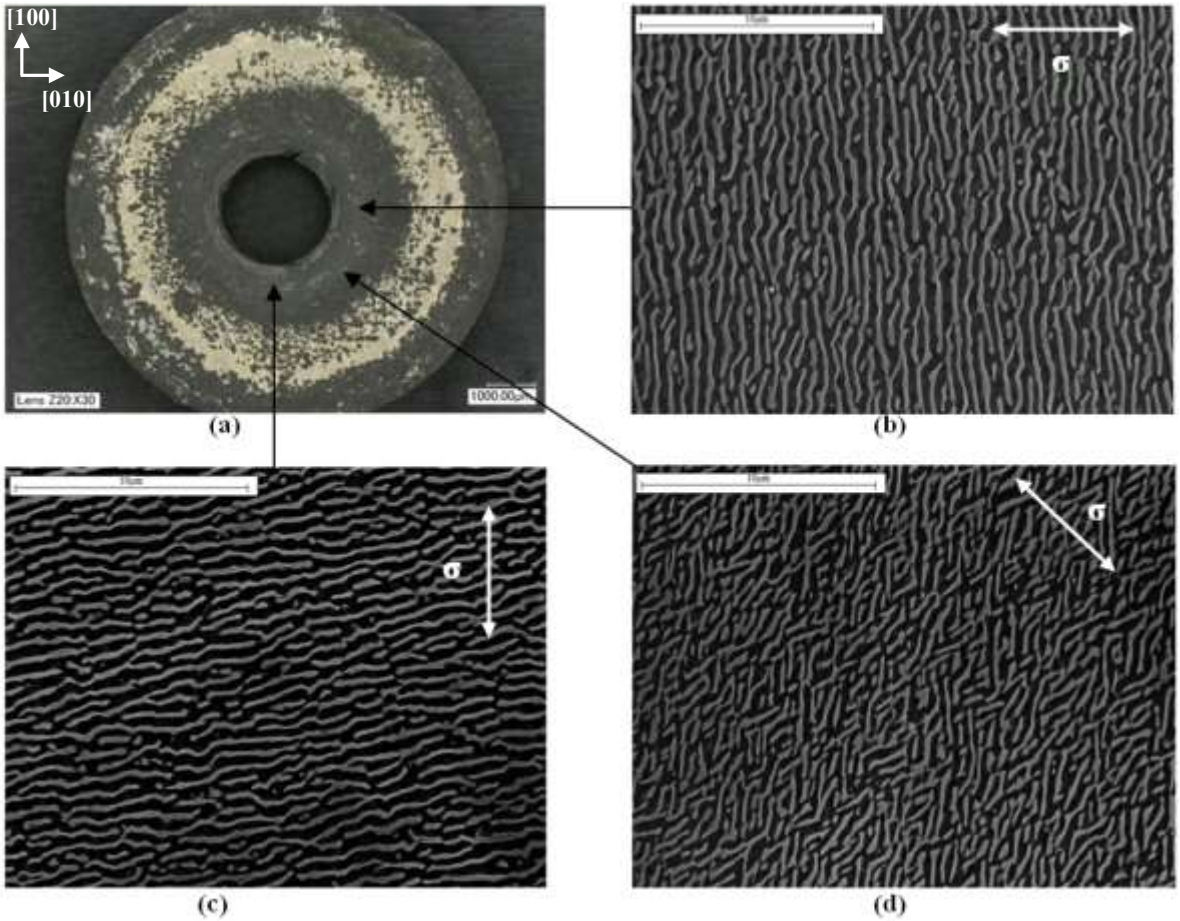

Figure 11 - Orthogonal Rafting due to biaxial tension deformation in a SP creep test (a) fractured SP specimen (b) longitudinal rafted microstructure (c) lateral rafted microstructure (d) orthogonal region of rafting regime

Furthermore, it is towards the centre of the disc that the most prominent rafting is observed due to the deformation of the material under the applied SP load being most prevalent. Conversely, within the clamped circular region of the test piece, no rafting takes place since no loading is acting upon it except that accumulated by thermal stresses.

Table 3 demonstrates how the microstructure of CMSX-4 evolves under high temperature creep exposure. Measurements of the γ/γ' phases were taken perpendicular to the rafting direction and approximately 2.5mm from the edge of the fractured SP discs. In each case, the calculations were achieved using three images taken at a magnification of 8000x and were then analysed through Gwyddion image analysis software [22], which utilises through pixel calibration. The rafting behaviour is seen to have two dependents, time and temperature. After a similar period of time at the different temperatures, rafting is found to coarsen to a greater extent at the higher temperatures. However, when a constant load is applied, thus resulting in different failure lives, time dependency affects the coarsening of the microstructure and the highest temperature may not result in the coarsest rafted microstructure, as is the case for 190N, where rafting is coarsest at 1050°C with a 61 hour life compared to 1150°C with a 4.25 hour life.

Table 3 - Microstructural Measurements of CMSX-4

	Constant SP Load (190N)		Similar failure lives (14-22 hours)	
Temperature (°C)	**Average width of γ' (µm)**	**Average width of γ channels (µm)**	**Average width of γ' (µm)**	**Average width of γ channels (µm)**
RT	0.45	0.15	0.45	0.15
950°C	0.322	0.199	No Rafting Present	
1050°C	0.466	0.393	0.336	0.196
1150°C	0.411	0.275	0.465	0.523

Post test microstructural analysis revealed that all 1050°C and 1150°C microstructures had experienced rafting and determined that the temperature dependence for rafting to occur was found to be at temperatures greater than 950°C. Whereas at 950°C, not all post test analysis of microstructures revealed rafting, thus leading to a temperature dependence. Figure 13Figure 12 demonstrates the proposed time and temperature dependence of the rafting regime in CMSX-4 through SP creep testing. The figure shows areas of: no rafting, semi-rafted microstructure, time dependent rafting and temperature dependent rafting. The principle of a semi-rafted microstructure is illustrated in Figure 13.

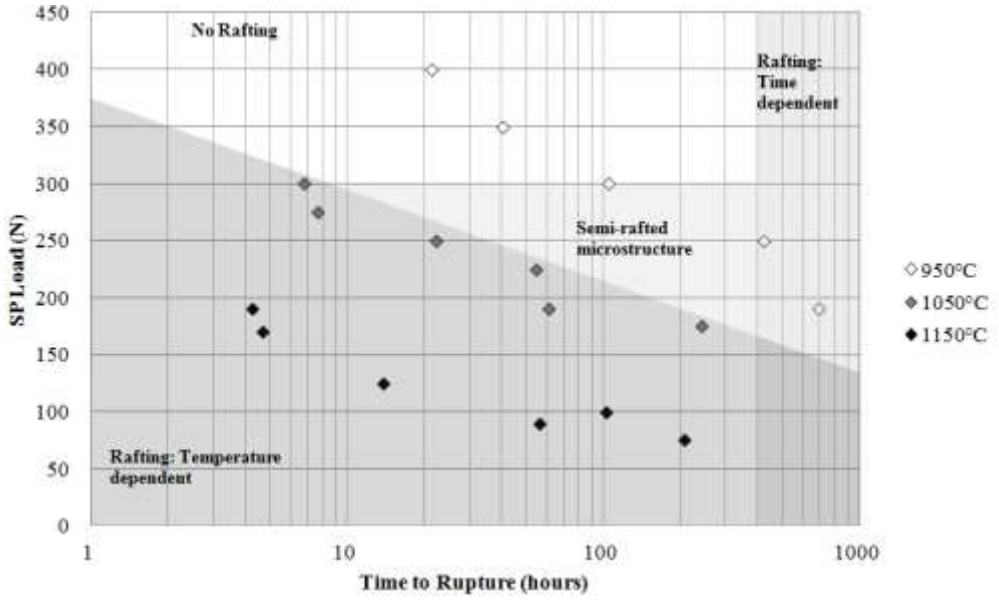

Figure 12 - SP load vs. Time to Rupture displaying the proposed time and temperature dependence of rafting

Figure 13 depicts the evolution of the rafting regime at 950°C. Figure 13(a) shows the microstructure after 41 hours under an applied load of 350N confirming very little rafting in which the cubic nature of γ' precipitates is still very visible, a time of 105 hours at 300N (figure 13(b) showing the initial stages of evolution of the cubic configuration into a rafting type morphology where the γ' particles begin to coalesce perpendicular to the load direction, and finally figure 13(c) which displays the microstructure after 422 hours at 250N, whereby a completely rafted structure is observed. It is suggested that this time dependence of rafting may account for the change in the k_{sp} factor from 0.6 at 950°C to 0.8 at 1050°C, since all microstructures at 1050°C are seen to be rafted. This raises the concept that the rafting regime may perhaps have a detrimental effect on the rupture life during a SP test.

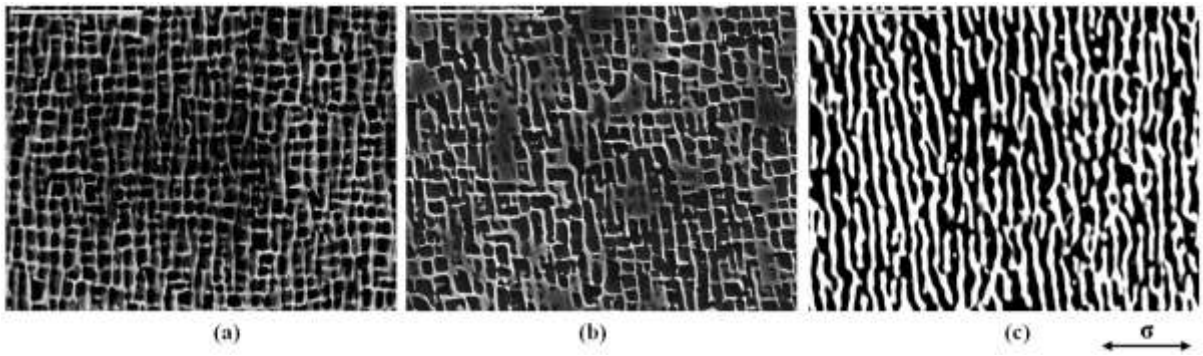

Figure 13 - Evolution of rafting in CMSX-4 at 950°C (a) 350N, 41 hours (b) 300N, 105 hours (c) 250N, 422 hours under SP loading

3.2. Fracture Mechanism

Figure 14 shows fractographic analysis of an SP creep test that was interrupted after 60 hours during the onset of tertiary deformation, where the nature of the biaxial tension state is evident. The image suggests that deformation occurs through four planes meeting at the point of contact where the indenter penetrates into the material, which is consistent with the highly crystallographic nature of single crystal material. Fracture then occurs with a ligament of CMSX-4 peeling away from the plane with the lowest critical resolved shear stress (CRSS).

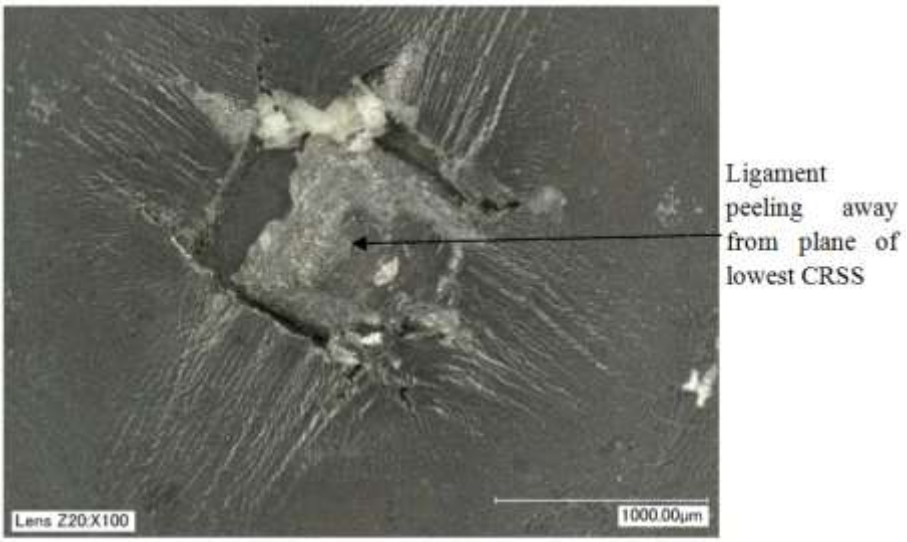

Figure 14 - Interrupted SP creep test at 1050°C and 200N

Figure 15 shows the profile of the fractured SP creep specimens at the three test temperatures; 950°C, 1050°C and 1150°C, for a similar time to rupture (a-c) and for a constant load of 190N (d-f). The ductility of each of the fractures is clear to see and appears to be consistent across temperatures and loads. In each case, the principle of deformation occurring through four perpendicular planes meeting at the centre of the SP disc can be seen as well as the peeling away of a ligament, which is more readily identifiable in some tests compared to others.

Future research into the SP creep response of CMSX-4 is worthwhile in order to investigate the anisotropic effects of the material both at elevated and lower intermediate temperatures. This will be achieved by applying the load such that the biaxial tension on the specimen is encompassed along the stronger [001] orientation and a secondary weaker orientation. Secondly, a comprehensive study into the application of creep life prediction models such as Larson-Miller and the Wilshire equations [23], [24] may be proven possible not just for CMSX-4 but for the SP creep test method itself.

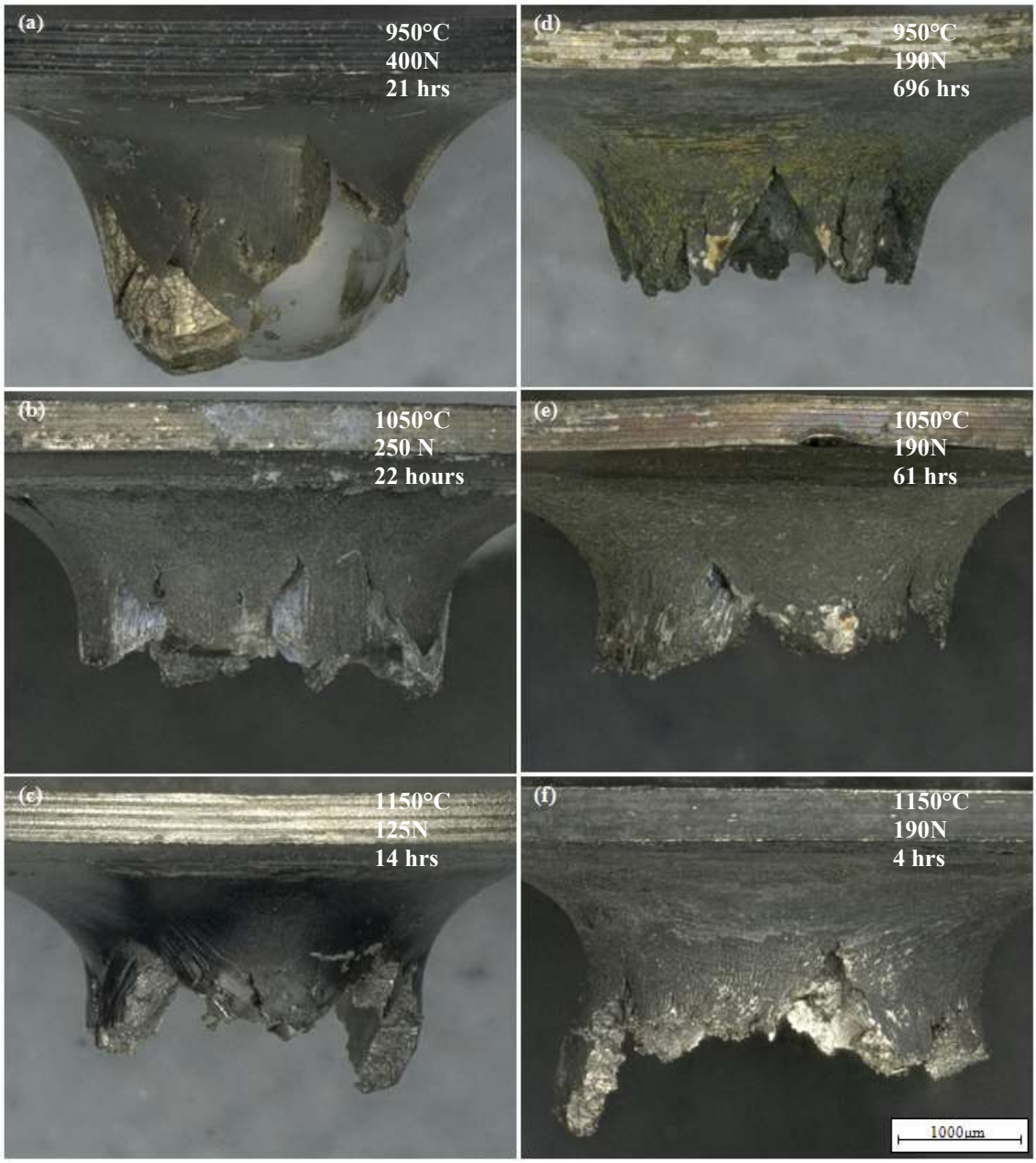

Figure 15 - Profile of fractured SP specimens for similar rupture times at (a) 950°C, (b) 1050°C and (c) 1150°C and a constant load of 190N at (d) 950°C, (e) 1050°C and (f) 1150°C.

4. Conclusions

This paper has assessed the suitability of applying the small punch creep test in determining the elevated temperature creep properties and fracture mechanism of the second generation single crystal superalloy, CMSX-4. Results have shown that data generated from the small punch test has the potential to be correlated to uniaxial creep results by using the K_{SP} method, despite the contrasting mechanisms of deformation. Furthermore, the small punch test was capable of revealing subtle microstructural changes in the rafting morphology of single crystals and how the microstructure evolves with a strong time and temperature dependence. However, even though a strong correlation between the two test approaches has been detailed, a more holistic understanding of the anisotropic effects of single crystals is required, particularly at lower intermediate temperatures, in order to produce a more representative relationship.

Acknowledgements

The current research was funded under the EPSRC Rolls-Royce Strategic Partnership in Structural Metallic Systems for Gas Turbines (grants EP/H500383/1 and EP/H022309/1). The provision of materials and technical support from Dr Neil Jones and Dr Duncan MacLachlan at Rolls-Royce plc. is gratefully acknowledged. The authors would also like to thank Dr. Mark Whittaker and Steve Williams for their help and advice in preparation of the manuscript.

References

[1] M. P. Manahan, A. S. Argon, and O. K. Harling, "The development of a miniaturizsed disk bend test for determination of post irradiation mechanical properties," *J. Nucl. Mater.*, vol. 104, pp. 1545–1550, 1981.

[2] F. Di Persio, G. C. Stratford, and R. C. Hurst, "Validation of the small punch test as a method for assessing ageing of a V modified low alloy steel," in *Baltica vi: life management and maintenance for power plants, vol 1 and 2*, 2004, pp. 523–535.

[3] D. Norris and J. D. Parker, "Deformation processes during disc bend loading," *Mater. Sci. Technol.*, vol. 12, no. February, 1996.

[4] CEN Workshop Agreement CWA 15267, "European Code of Practise: Small Punch Test Method for Metallic Materials." 2007.

[5] V. Bicego, F. Di Persio, R. C. Hurst, and G. C. Stratford, "Comparibility of Results Via the Miniaturised Small Punch Test Method and Traditional Uniaxial Creep Testing," in *11th International Conference on Fracture*, 2005, pp. 4808–4814.

[6] E. C. Moreno-Valle, W. Pachla, M. Kulczyk, B. Savoini, M. A. Monge, C. Ballesteros, and I. Sabirov, "Anisotropy of uni-axial and bi-axial deformation behavior of pure Titanium after hydrostatic extrusion," *Mater. Sci. Eng. A*, vol. 588, pp. 7–13, Dec. 2013.

[7] C. Rodriguez, J. Cabezas, E. Cardenas, F. Belzunce, and C. Betegon, "Mechanical Properties Characterization of Heat-Affected Zone Using the Small Punch Test," *Weld. Journal2*, vol. 88, pp. 188–192, 2009.

[8] K. Turba, R. C. Hurst, and P. Hähner, "Anisotropic mechanical properties of the MA956 ODS steel characterized by the small punch testing technique," *J. Nucl. Mater.*, vol. 428, no. 1–3, pp. 76–81, Sep. 2012.

[9] V. Bicego, J. H. Rantala, J. Klaput, G. C. Stratford, F. Di Persio, and R. C. Hurst, "The Small Punch Test Method: Results from a European Creep Testing Round Robin," in *4th International Conferences in Advances in Materials Technology for Fossil Power Plants*, 2004.

[10] R. J. Lancaster, R. C. Hurst, G. Norton, M. R. Bache, and J. Lindemann, "Small Punch Creep Testing of Next Generation TiAl Alloys," in *3rd International European Creep Collaborative Committee on Creepo and Fracture*, 2014.

[11] R. . Hurst, R. Lancaster, G. Norton, R. Banik, and M. R. Bache, "A Renaissance in Small Punch Testing at Swansea University," in *Fast tools for condition and life assessment of power plants*, 2013.

[12] P. Caron, Y. Ohta, Y. G. Nakagawa, and T. Khan, "Creep deformation anisotropy in single crystal superalloys," *Superalloys*, pp. 215–224, 1988.

[13] C. Knobloch, S. Volker, D. Sieborger, and U. Glatzel, "Anisotropic creep behavior of a nickel-based superalloy compared with single phase nickel solid solution and y' phase single crystals," *Mater. Sci. Eng. A*, pp. 237–241, 1997.

[14] V. Sass, U. Glatzel, and M. Feller-Kniepmeier, "Anisotropic creep properties of the nickel-base superalloy CMSX-4," *Acta Mater.*, vol. 44, no. 5, pp. 1967–1977, May 1996.

[15] T. E. García, C. Rodríguez, F. J. Belzunce, and C. Suárez, "Estimation of the mechanical properties of metallic materials by means of the small punch test," *J. Alloys Compd.*, vol. 582, pp. 708–717, Jan. 2014.

[16] W. Hermann, H. G. Sockel, J. Han, and A. Bertram, "Elastic properties and determination of elastic constants of nickel-base superalloys by a free-free beam technique," *Superalloys*, pp. 229–238, 1996.

[17] A. Royer, P. Bastie, and M. Veron, "In situ determination of γ′ phase volume fraction and of relations between lattice parameters and precipitate morphology in Ni-based single crystal superalloy," *Acta Mater.*, vol. 46, no. 15, pp. 5357–5368, Sep. 1998.

[18] R. C. Reed, *The Superalloys: Fundamentals and Applications*. Cambridge University Press, 2006, pp. 180–186.

[19] R. C. Reed, N. Matan, D. C. Cox, M. A. Rist, and C. M. F. Rae, "Creep of CMSX-4 superalloy single crystals: effects of rafting at high temperature," *Acta Mater.*, vol. 47, no. 12, pp. 3367–3381, Sep. 1999.

[20] R. Giraud, J. Cormier, Z. Hervier, D. Bertheau, K. Harris, J. Wahl, X. Milhet, J. Mendez, and A. Organista, "Effect of the prior microstructure degradation on the high temperature/low stress non-isothermal creep behavior of cmsx-4® Ni-based single crystal superalloy," in *Superalloys*, 2012.

[21] D. Chatterjee, N. Hazari, N. Das, and R. Mitra, "Microstructure and creep behavior of DMS4-type nickel based superalloy single crystals with orientations near 〈001〉 and 〈011〉," *Mater. Sci. Eng. A*, vol. 528, no. 2, pp. 604–613, Dec. 2010.

[22] http://www.gwyddion.net/, "Gwyddion." .

[23] F. R. Larson and J. Miller, "A Time-Temperature Relationship for Rupture and Creep Stresses," *Trans. ASME*, vol. 74, pp. 765–775, 1952.

[24] M. T. Whittaker and B. Wilshire, "Advanced Procedures for Long-Term Creep Data Prediction for 2.25 Chromium Steels," *Metall. Mater. Trans. A*, vol. 44, no. S1, pp. 136–153, Apr. 2012.